AGU ADVANCING EARTH AND SPACE SCIENCES

Geophysical Research Letters

RESEARCH LETTER
10.1029/2023GL105424

A New Approach for Real-Time Erupted Volume Estimation From High-Precision Strain Detection Validated by Satellite Topographic Monitoring

Alessandro Bonaccorso[1], Luigi Carleo[1], Gilda Currenti[1], Giuseppe Bilotta[1], Annalisa Cappello[1], and Gaetana Ganci[1]

[1]Istituto Nazionale di Geofisica e Vulcanologia – Osservatorio Etneo, Catania, Italy

Key Points:

- Detection of strain changes during sequences of lava fountain eruptions from continuous recording high-precision borehole instruments
- Quantifying erupted volumes from strain changes, comparison and validation with the volumes calculated from high spatial resolution satellite measurements
- New method to estimate the erupted volumes in real-time by using the continuous strain recording

Supporting Information:

Supporting Information may be found in the online version of this article.

Correspondence to:

A. Bonaccorso,
alessandro.bonaccorso@ingv.it

Citation:

Bonaccorso, A., Carleo, L., Currenti, G., Bilotta, G., Cappello, A., & Ganci, G. (2023). A new approach for real-time erupted volume estimation from high-precision strain detection validated by satellite topographic monitoring. *Geophysical Research Letters*, *50*, e2023GL105424. https://doi.org/10.1029/2023GL105424

Received 10 JUL 2023
Accepted 22 OCT 2023

Author Contributions:

Conceptualization: Alessandro Bonaccorso, Gilda Currenti
Data curation: Luigi Carleo, Gilda Currenti
Funding acquisition: Alessandro Bonaccorso
Investigation: Alessandro Bonaccorso, Annalisa Cappello, Gaetana Ganci
Methodology: Alessandro Bonaccorso, Luigi Carleo, Gilda Currenti, Giuseppe Bilotta, Annalisa Cappello, Gaetana Ganci

Abstract Timely estimations of magma volumes emitted during an eruption or a sequence of explosive events are vital for investigating the eruptive activity and evaluating the associated hazard. A reliable method for estimating erupted volumes is based on the analysis of digital surface models that nowadays can be obtained subsequently using stereo or tri-stereo optical satellite imagery. However, the real-time estimation of the erupted volumes is still an open challenge. Here, we explore the capacity of extracting volume estimates from continuous measurements of volumetric strain changes recorded by borehole dilatometers. We compare the volumes derived from numerous high spatial resolution satellite images with high precision strain records at Etna during 2020–2022, when more than 60 lava fountains occurred. The good correlation between the two data sets shows that strain changes can be used as a proxy to estimate the emitted volumes both over time and in real-time.

Plain Language Summary Quantifying erupted volumes is fundamental in volcanology to provide a robust characterization of eruptions. To date, estimates of erupted volumes have been calculated after the eruptions have ended and the real-time estimation of the erupted volumes is still an on-going challenge. In recent decades, the sequences of lava fountain-type eruptions at Etna, with dozens of episodes close in time and more than 100 episodes occurring since 2011, has made the task of estimating the volumes in real-time during each single eruption ever more essential. This would enable providing precise information to Civil Protection authorities and contribute toward hazard evaluation. In this study, we took on this new challenge by exploring the potential to extract erupted volume estimates from continuous measurements of strain changes, recorded by high-precision borehole instruments installed on the volcano's flanks. We compared and validated the volumes deriving from numerous high spatial resolution satellite images with high-precision strain records at Etna during 2020–2022, when more than 60 lava fountains occurred. The good correlation between the two data sets shows that strain changes can be used effectively as a proxy to estimate the emitted volumes, both over time and, more importantly, in real-time.

1. Introduction

Quantification of erupted volumes is a fundamental task in volcanology to provide a robust characterization of the eruptions. Several methods have been proposed to infer eruptive volumes by eruptive deposits estimation (e.g., Engwell et al., 2015 and references therein), which is of key importance especially for reconstructing large explosive eruptions in the past. For explosive events, under the assumption of a fixed cylinder diameter for the conduit, the volumes of pyroclasts can be obtained by measuring the outflow velocity of the fluid from the analysis of thermal camera images. This indirect method has been applied at Etna (e.g., Calvari & Nunnari, 2022a and reference therein). However, it only provides an estimation of the explosive pyroclastic portion without furnishing information on the effusive portion, associated with the lava overflows, which are usually present in the explosive activity of the basaltic volcanoes.

Another way to calculate the volume associated with lava fountains is by using geostationary satellite imagery that, given the high revisit time, provides precise information on the lava flow cooling and, hence, can be modeled to infer the lava volume (Ganci et al., 2012). Even if this technique is consolidated for lava fountains at Mt. Etna (Bonaccorso et al., 2011; Ganci et al., 2018, 2023b), geostationary satellites cannot accurately measure the pyroclastic volume that cools in a very short time compared to lava. Nowadays, a more accurate and reliable approach to calculate the total erupted volume is provided by the topographic comparison astride the investigated eruptive

Project Administration: Alessandro Bonaccorso
Software: Luigi Carleo, Giuseppe Bilotta
Supervision: Alessandro Bonaccorso
Validation: Gilda Currenti, Annalisa Cappello, Gaetana Ganci
Visualization: Luigi Carleo
Writing – original draft: Alessandro Bonaccorso, Luigi Carleo, Gilda Currenti, Annalisa Cappello, Gaetana Ganci

period. 3D morphology of volcanic edifices can be regularly updated thanks to on-demand very high-resolution optical satellite imagery acquired in stereo, tri-stereo or multi-view configurations. This satellite imagery can produce the topographic monitoring of Earth surface by applying photogrammetry techniques to build digital surface models (DSMs). By differencing successive DSMs before and after an eruptive period, an estimation of the erupted bulk volumes made up of the sum of lava flows plus the pyroclastic deposits emplaced can be derived. This approach is extremely useful for infrequent eruptive events; however, depending on the passage of satellites and subsequent data processing, the volume estimation has a time delay usually of days and it is not suitable for near real-time purposes.

At Etna in recent decades, sequences of numerous lava fountain events have occurred in a short time (up to dozens of events in a few months), which requires monitoring and multidisciplinary data analysis in real-time. These explosive eruptions are short-lasting events, with mean durations from tens of minutes to several hours, ejecting lava fragments to heights of hundreds of meters. Lava fountains form high eruptive columns causing plume dispersal and ash fallout that can mean hazards for civil aviation and infrastructures of the urban areas (Calvari et al., 2018 and references therein). The eruptive activity is also accompanied by effusive lava flows that usually remain confined in the upper sectors of the volcano. Therefore, the total erupted volume is made up of the explosive pyroclastic portion and the effusive one. The high rate of temporal occurrence of these eruptive events can produce and cumulate large magma volumes over time.

A typical lava fountain produces small deformation ($\leq$1 microstrain; Bonaccorso et al., 2013), difficult to detect with classic geodetic techniques such as GPS and InSAR. An effective technique to monitor lava fountains is the high-precision borehole dilatometer since it measures the volumetric strain in a wide frequency range (from 10^{-7} to more than 20 Hz) and with the highest resolution (order of 10^{-10}) achievable among geophysical instruments (i.e., NASEM, 2017; Roeloffs & Linde, 2007). These characteristics make the dilatometer strategic for real-time monitoring and surveillance of rapid events such as the lava fountains (Bonaccorso et al., 2021; Carleo, Currenti, et al., 2022; Carleo et al., 2023). The high-precision strain recorded by borehole dilatometers is able to detect the decompression of the source that fuels the lava fountain (e.g., Bonaccorso et al., 2016; Roeloffs & Linde, 2007). The recorded changes are proportional to the volume variation of the magmatic plumbing system feeding the eruption, and therefore are related to the total erupted volume. Thanks to the continuous monitoring of the strain provided by the dilatometers, this relation can be exploited to estimate erupted volumes in real-time.

In this work, we compare volumes derived from DSMs differencing and strain change measurements to verify the relationship between emitted volumes and strain variations.

We have made the most of the extraordinary intense Etna activity between 13 December 2020 and 21 February 2022, when more than 60 lava fountain events (Calvari & Nunnari, 2022a; Carleo et al., 2023; Ganci, Bilotta, et al., 2023) occurred. This high number of explosive eruptions represents an exceptional set of events which has enabled collecting a vast amount of information never previously recorded in a short time, both in terms of satellite remote sensing for DSMs production and ground deformation recorded by high-precision borehole dilatometers.

In Section 2, we briefly describe the lava fountain sequence that occurred in 2020–2022. In Section 3, we introduce the satellite topographic approach for DSMs comparison. In Section 4, we present the high-precision strain changes recorded by the borehole dilatometer and the data processing to reveal the ultra-small changes. Finally, we compare the volumes obtained by successive DSMs comparison and the ones deduced by strain changes. We propose a new method that can provide robust information on the erupted volumes both over time and in real-time through the strain changes recorded by continuous monitoring.

2. Etna 2020–2022 Lava Fountains Sequence

Lava fountains are generated when a large volume of volatiles rapidly exsolves from the magma during its ascent. The subsequent fast decompression along the upper plumbing system causes the mixture of gas and pyroclasts to rise rapidly from the vent as a jet (i.e., Wilson et al., 1995), expanding vertically into an eruptive column. The lowest portion of this column comprises the lava fountain (i.e., Sparks et al., 1997; Bonaccorso & Calvari, 2017). Above it, a convective region forms that can reach 10–15 km height, followed by wind-driven ash transport of hundreds of kilometers (i.e., Carey & Sparks, 1986; Calvari et al., 2018).

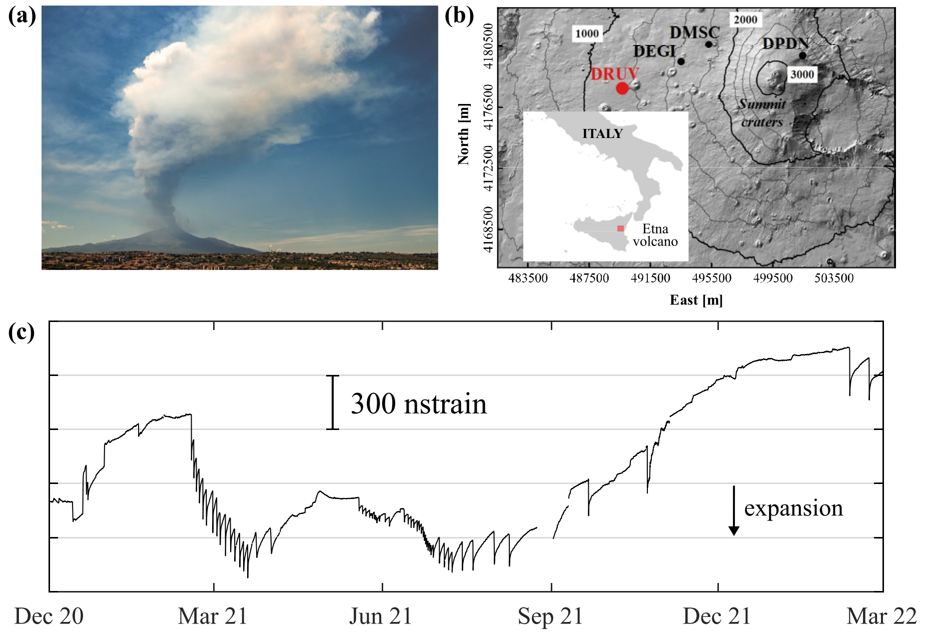

Figure 1. (a) Lava fountain at Etna on 16 June 2021 (photo courtesy of Francesco Zuccarello). (b) Location of the strainmeters installed on Etna. The red dot indicates the recording station DRUV used in this study. (c) Filtered strain signal during the study period. The "saw teeth" marking the signal are the strain changes recorded during the lava fountain episodes.

At Etna volcano, lava fountains reach heights of hundreds of meters, lasting from tens of minutes to several hours, and generate both a portion of volume caused by the pyroclastic fall-out accumulation and a portion of volume feeding lava flows, which can reach maximum lengths of 4–6 km (i.e., Calvari et al., 2011, 2018; Ganci et al., 2012, 2013). The majority of the lava fountains have a mean duration of ∼2 hr and sustain lava jets with mean heights of 500–1,000 m (Figure 1a).

After a two-year recharge phase, following the brief flank eruption of December 2018 (Aloisi et al., 2020; Cappello et al., 2022), a lava fountain sequence began on 13 December 2020, heralded by three seismic swarms occurring during the two weeks before (Bonaccorso et al., 2021; Calvari et al., 2022). More than 60 lava fountains were erupted from summit SE crater (SEC) until 21 February 2022. Despite a general similitude of the single lava fountains, these can have different characteristics, namely magnitude (i.e., erupted volume) and intensity (i.e., mass eruption rate), and depending on these features the different episodes can have a different impact in terms of associated hazard. Calvari and Nunnari (2022b) analyzed all the lava fountain episodes from 2020 to 2022 using the images recorded by the monitoring network of thermal cameras. They found a high variability in the pyroclastic volume erupted during the different eruptive episodes.

Calvari et al. (2022) selected three different episodes occurring between 13 December 2020 and 12 March 2021, and analyzed the data from a multidisciplinary perspective by considering terrestrial cam and Satellite SEVIRI images, seismic, infrasound, and strain data. A high variability of both volcanological (pyroclastic and lava flow volumes, eruption rate) and geophysical (seismic, infrasound and strain amplitudes and strain rate) parameters was observed. Carleo et al. (2023) applied an unsupervised machine learning algorithm to characterize all the strain changes associated with the lava fountains in 2020–2022. They found that the amplitude of a strain variation, which is related to the total erupted volume, is one of the signal features that characterizes a lava fountain. In Figure 1c, the filtered strain signal during the study period is presented. All the negative step-like strain variations occurred concurrently with lava fountains.

3. Satellite DSMs Method and Strain Comparison

In order to quantify the volumes of volcanic deposits emplaced at Etna, we exploited high spatial resolution stereo WorldView and tri-stereo Pléiades acquisitions recorded between August 2020 and June 2022. In particular, we used six different acquisitions, namely five Pléiades triplets acquired on 18 July 2016

Table 1
Volumes Obtained From DSMs Difference and Sums of the Strain Variations Recorded at the DRUV Dilatometer Borehole Station for Different Time Intervals During the SEC Lava Fountains of 2020–2022

Time intervals	Number of lava fountains	Volume from DSMs difference [10^6 m^3]	Cumulated strain [nstrain]
22 Aug 2020–26 Feb 2021	13	24.5	1,692.4
26 Feb 2021–27 Jul 2021	47	63.3	4,113.4
13 Jul 2021–27 Jul 2021	2	4.26	325.7
22 Aug 2020–27 Jul 2021	60	85.9	5,805.8
27 Jul 2021–29 Jun 2022	7	20.49	1,465.5
26 Feb 2021–29 Jun 2022	54	81.5	5,578.8
22 Aug 2020–29 Jun 2022	67	103.53	7,271.3

(Cappello et al., 2019), 22 August 2020, 26 February 2021, 13 July 2021, 27 July 2021, and 29 June 2022 (Ganci, Bilotta, et al., 2023), and a stereo pair WorldView-1 acquired on 27 July 2021 (Ganci, Cappello, & Neri, 2023). The Pléiades and WorldView imagery were processed using the free and open source MicMac photogrammetric library (http://micmac.ensg.eu) developed by the French Institut Géographique National, which consists of three main steps: (a) tie points recognition and matching between images; (b) calibration and orientation, assessing relationships between viewpoints and objects; (c) correlation, producing dense matching for 3D scene reconstruction. The resulting DSMs have a horizontal resolution of 1 m and an average vertical accuracy, estimated by using GPS Ground Control Points (Ganci et al., 2019) outside the area covered by the volcanic deposits, of about 1.2–1.4 m.

In order to obtain more reliable height differences and minimize the errors due to misalignments, we performed pairwise co-registrations by applying the Nuth and Kääb algorithm, which finds the horizontal and vertical shifts between the DSMs using the slope-aspect method and removes them (Nuth & Kääb, 2011). After this, along/cross track corrections are then determined and applied. By making pairs of DSM differences, we obtained the topographic changes due to the emplacement of volcanic deposits separately in seven time windows: (a) from 22 August 2020 to 26 February 2021, (b) to 27 July 2021 and (c) to 29 June 2022, (d) from 26 February 2021 to 27 July 2021 and (e) to 22 June 2022, (f) from 13 to 27 July 2021, (g) and from 27 July 2021 to 29 June 2022 (Table 1). The total volume of products was calculated by integrating the thickness distribution over the area covered by the deposits (Figure 2a), while the uncertainty was quantified as the product of the area and the standard deviation of terrain residuals outside of the deposits (Figure 2b).

4. Strain Recording

In the last decade, Sacks-Evertson strainmeters (Sacks et al., 1971) were installed on Etna to monitor ground deformation induced by the volcano activity (Figure 1b). These instruments are installed in drilled holes (depth >100 m) to reduce the environmental noise and are coupled with rock with expansive cement. The strainmeters recorded changes during the lava fountain events (i.e., Bonaccorso et al., 2021). In this work, we focused on the measurements recorded by the DRUV strainmeter located ∼10 km away from the Etna summit craters (installation depth of ∼180 m) and optimally coupled with a massive rock layer characterized by a high efficiency in transferring deformation, making it the station with the best response and accuracy in the strainmeters network (Bonaccorso et al., 2016; Currenti et al., 2017).

The recorded strain signal is usually affected by disturbing signal components that could mask the deformation induced by the volcanic activity (Currenti & Bonaccorso, 2019). To unravel the strain variations caused by the eruptive episodes, appropriate signal filtering operations must be performed. We used the protocol developed by Carleo, Bonaccorso, et al. (2022) to efficiently filter the effects of the main disturbing sources of the strain signal, namely the atmospheric pressure and the Earth's tides (10^{-7} to 10^{-8}), and reveal ultra-small volcano-related strain changes up to 10^{-10} that can be partially masked in the recorded signal (Figures 3a and 3b). The strain variation identified concurrently with an eruptive event is the response of the rock to the decompression of a magmatic

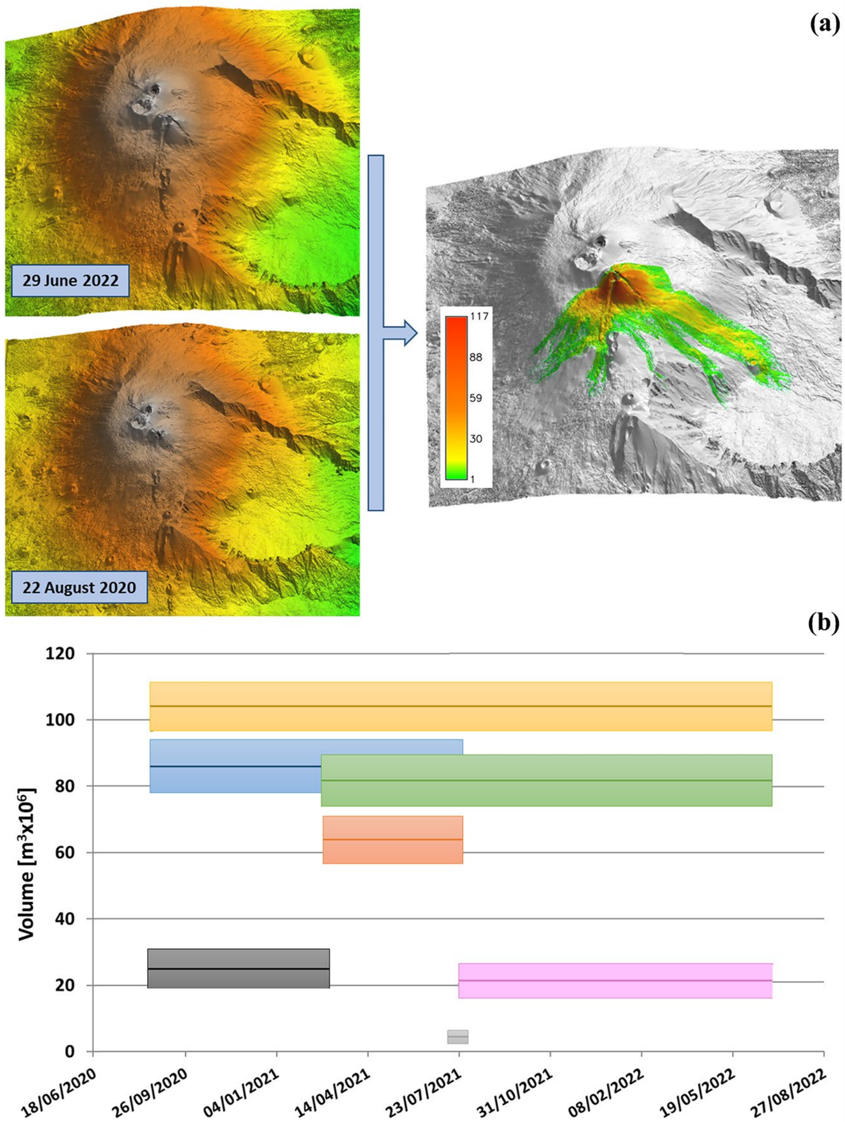

Figure 2. (a) Height difference (in meters) between the DSMs derived from satellite images acquired on 29 June 2022 and 20 August 2020 related to the SEC lava fountains. (b) Volumes and relative uncertainties (colored bars) computed from DSM difference from August 2020 to June 2022. Uncertainties are estimated by multiplying the area and the standard deviation of terrain residuals outside of the deposits.

source feeding the eruption and thus represents a crucial quantity that can be related to the total erupted volume. An example of strain variation related to the lava fountains is shown in Figure 3c. The strain signal reflects the evolution of the eruption showing a decreasing trend that gradually increases its slope until the signal reaches a minimum value corresponding to the end of the eruption (Carleo et al., 2023). The amplitude of the strain variation can be estimated as the difference between the strain value at the onset (red circle in Figure 3c) and the strain value at the ending time (black circle) of the variation. For a robust picking, we developed an automatic procedure based on the method of Carleo, Currenti, et al. (2022), which is able to detect the onset and the end of the strain change by a 20-min moving window in which the standard deviation of the signal is calculated and compared with the background level. With this procedure, we can estimate the amplitude of each variation with an uncertainty of 0.13 nstrain (more details in Text S1 in Supporting Information S1). The onset, the end and the amplitude of all the strain variations recorded during the lava fountain episodes, are reported in Table S1 in Supporting Information S1.

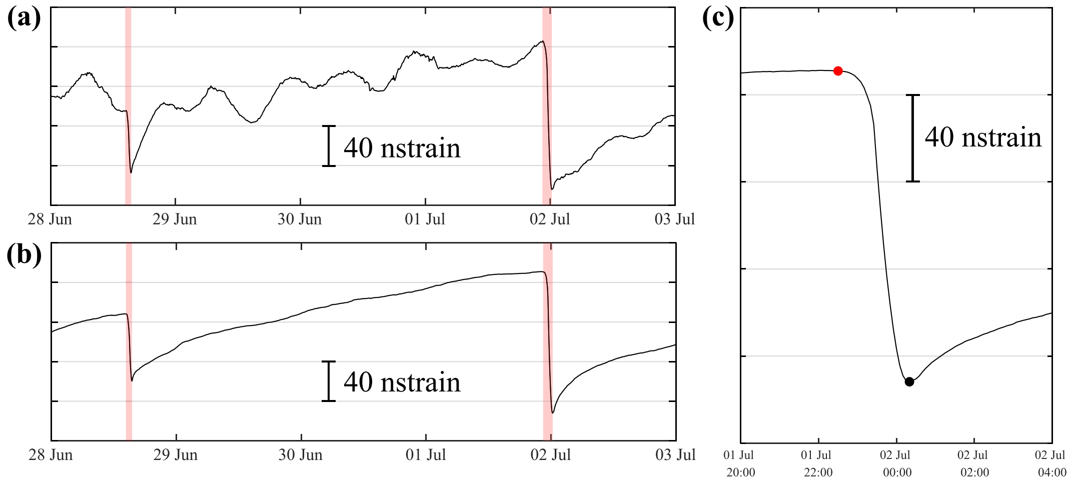

Figure 3. (a) Recorded and (b) filtered DRUV strain signal in the period 28 June–03 July 2021, when two lava fountains occurred (red shaded areas). (c) Zoom of the lava fountain on 01–02 July 2021. The red and black circles correspond to the onset and the ending time of the variation, respectively.

The strain variations of the lava fountains were summed for the single values associated with the events contained in each of the seven time intervals in which the erupted volume difference was calculated from the comparison of the DSMs (Table 1). The linear relationship between total erupted volume computed from DSM differences and volumetric strain measured by the borehole dilatometer for the analyzed time periods is shown in Figure 4.

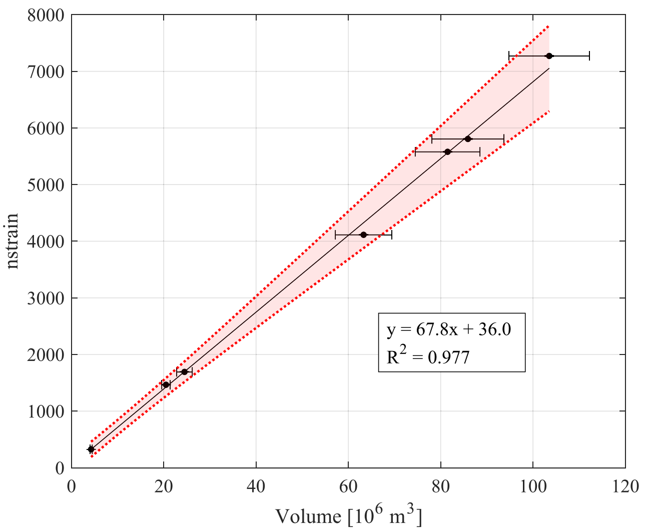

Figure 4. Linear relationship between the total erupted volume computed from the satellite DSMs difference and the volumetric strain measured by the borehole dilatometer for the analyzed time periods. The fit was obtained with the regression method of Mahon (1996). We found a slope of 67.8 ± 3.1 and an intercept of 36.0 ± 57.4, with a goodness of fit (R^2) of 0.977. Dashed lines indicate the 95% confidence interval.

5. Discussion and Conclusion

Depending on the quantity of erupted magma volume, the lava fountains have a major impact on the territory since ash plumes travel beyond the volcano area and the subsequent ash fallout can cause air traffic problems, often the closure of airports (in particular the international airport of Catania, the busiest in southern Italy), as well as disruptions in road traffic. It is thus a primary scientific target to evaluate the impact of these eruptive events based on parameters recorded by the monitoring networks.

The estimate of the volumes erupted is usually calculated a-posteriori, after the conclusion of the eruptions. In recent decades, the sequences of lava fountain-type eruptions at Etna, with the episodes close in time, posed the challenge to estimate the volumes in real-time during each single eruption, to provide precise information to Civil Protection authorities. In volcanoes with frequent eruptive activity, this issue is of fundamental importance, since the evaluation of erupted volumes during the eruption allows for a better characterization of the event, contributing to the complete evaluation of the associated hazard.

Bonaccorso et al. (2013) had implemented an indirect method to constrain the volume emitted by the 2011–2013 lava fountains from SEC by modeling the source that caused the strain recorded during these eruptions. The authors modeled the average strain recorded during the lava fountains by using a finite element method (FEM) approach. They found that a shallow prolate source, with an aspect ratio of 0.5, at depth of 0 km b.s.l. and a change of volume of 2×10^6 m^3 is able to reproduce the observed strain. The total emitted magma volume was estimated as the volume change of the source plus a small portion of $\sim 0.5 \times 10^6$ m^3 accommodated before each lava fountain due to the magma compressibility (Bonaccorso et al., 2013). This source has been interpreted as a small storage zone where gas-rich magma is trapped before being violently expelled thereby generating the lava fountains. The stability of the source depth over time was analyzed by using a Finite Element Method approach indicating that the centroid of its position is constrained in the range depth of 0.5–1 km b.s.l. (Bonaccorso et al., 2021). Moreover, this depth is consistent with the result obtained from the seismic tomography, revealing that in this range a shallow anomaly is present and interpreted as a volcanic source (De Gori et al., 2021).

Considering that for the 2011–2013 lava fountains the mean strain at DRUV was ∼150 nanostrain, then from the modeling result the conversion coefficient resulted ∼60 nanostrain per million cubic meters of erupted magma. This coefficient represents the strain response at DRUV site to the contraction of the modeled source occurring during the magma emission of lava fountains from SEC. In the past, this coefficient was used for first estimates of the volume emitted during the January 2011–December 2013 lava fountain sequence. Bonaccorso and Calvari (2013) for the first 38 lava fountains of the 16-month period January 2011–April 2013, estimated a total erupted volume of $\sim 95 \times 10^6$ m^3. In terms of hazard, this allowed to rightly affirm before the conclusion of the sequence that the lava fountain sequence represented an efficient way to release the magma stored within the supply system and, in that framework, it did not represent a precursor of major effusive events and, instead, favored the equilibrium of the volcano supply system.

Bonaccorso et al. (2021) found close similarities between the 2011–2012 and the 2020–2021 eruptive episodes, both in the position of the strain source and in the magma volume emitted during a lava fountain event. This aspect confirmed that the source propelling the lava fountains from SEC maintained the same position during both sequences.

The previous coefficient was obtained from an indirect method based on the modeling of the deformation effects of the source constrained by the solution from the FEM numerical method, and it can be considered a first estimation. In this study instead, we have considered a new approach that is independent of models, which, even if advanced, may suffer from limitations with respect to the complexity of the eruptive phenomena. We have investigated the direct comparison with volume values measured through the DSMs comparison technique during the 2020–2022 lava fountains sequence. This approach provides a coefficient of 67,8 nanostrain per million cubic meters of erupted magma as strain response at DRUV during a lava fountain from the SEC. Our results demonstrate the strict relationship between precise estimates of erupted volumes from periodic measurements of satellite remote sensing, and estimates from high-precision strain recorded in real-time during the lava fountains at Etna.

Data Availability Statement

Strain raw data of this study are available from Bonaccorso et al. (2023). Pléiades imagery is available through the Mt Etna supersite initiative at http://geo-gsnl.org/supersites/permanent-supersites/mt-etna-volcano-supersite-new/. MicMac photogrammetry software (Rupnik et al., 2017) is freely available.

Acknowledgments

This research benefited from funding provided the EC H2020- FET OPEN project "SiC nano for picoGeo," grant agreement No. 863220. This work was partially supported by the INGV project Pianeta Dinamico (CUP D53J19000170001) funded by MIUR ("Fondo finalizzato al rilancio degli investimenti delle amministrazioni centrali dello Stato e allo sviluppo del Paese," legge 145/2018), Tema 8—PANACEA and SAFARI.

References

Aloisi, M., Bonaccorso, A., Cannavò, F., Currenti, G., & Gambino, S. (2020). The 24 December 2018 eruptive intrusion at Etna volcano as revealed by multidisciplinary continuous deformation networks (CGPS, borehole strainmeters and tiltmeters). *Journal of Geophysical Research: Solid Earth*, *125*(8), e2019JB019117. https://doi.org/10.1029/2019JB019117

Bonaccorso, A., Bonforte, A., Calvari, S., Del Negro, C., Di Grazia, G., Ganci, G., et al. (2011). The initial phases of the 2008-2009 Mt. Etna eruption: A multi-disciplinary approach for hazard assessment. *Journal of Geophysical Research*, *116*(B3), B03203. https://doi.org/10.1029/2010JB007906

Bonaccorso, A., & Calvari, S. (2013). Major effusive eruptions and recent lava fountains: Balance between erupted and expected magma volumes at Etna volcano. *Geophysical Research Letters*, *40*(23), 6069–6073. https://doi.org/10.1002/2013GL058291

Bonaccorso, A., & Calvari, S. (2017). A new approach to investigate an eruptive paroxysmal sequence using camera and strainmeter networks: Lessons from the 3–5 December 2015 activity at Etna volcano. *Earth and Planetary Science Letters*, *475*, 231–241. https://doi.org/10.1016/j.epsl.2017.07.020

Bonaccorso, A., Carleo, L., Currenti, G., & Sicali, A. (2021). A. magma migration at shallower levels and lava fountains sequence as revealed by borehole dilatometers on Etna Volcano. *Frontiers in Earth Science*, *9*, 740505. https://doi.org/10.3389/feart.2021.740505

Bonaccorso, A., Currenti, G., Carleo, L., & Sicali, A. (2023). Strain data at DRUV borehole dilatometer from December 2020 to March 2022 at Etna volcano (version 3) [Dataset]. figshare. https://doi.org/10.6084/m9.figshare.24125763.v3

Bonaccorso, A., Currenti, G., Linde, A. T., & Sacks, S. I. (2013). New data from borehole strainmeters to infer lava fountain sources (Etna 2011–2012). *Geophysical Research Letters*, *40*(14), 3579–3584. https://doi.org/10.1002/grl.50692

Bonaccorso, A., Linde, A. T., Currenti, G., Sacks, S. I., & Sicali, A. (2016). The borehole dilatometer network of mount Etna: A powerful tool to detect and infer volcano dynamics. *Journal of Geophysical Research: Solid Earth*, *121*(6), 4655–4669. https://doi.org/10.1002/2016JB012914

Calvari, S., Biale, E., Bonaccorso, A., Cannata, A., Carleo, L., Currenti, G., et al. (2022). Explosive paroxysmal events at Etna Volcano of different magnitude and intensity explored through a multidisciplinary monitoring system. *Remote Sensing*, *14*(16), 4006. https://doi.org/10.3390/rs14164006

Calvari, S., Cannavò, F., Bonaccorso, A., Spampinato, L., & Pellegrino, A. G. (2018). Paroxysmal explosions, lava fountains and ash plumes at Etna Volcano: Eruptive processes and hazard implications. *Frontiers of Earth Science*, *6*, 107. https://doi.org/10.3389/feart.2018.00107

Calvari, S., & Nunnari, G. (2022a). Comparison between automated and manual detection of lava fountains from fixed monitoring thermal cameras at Etna Volcano, Italy. *Remote Sensing*, *14*(10), 2392. https://doi.org/10.3390/rs14102392

Calvari, S., & Nunnari, G. (2022b). Etna output rate during the last decade (2011–2022): Insights for hazard assessment. *Remote Sensing*, *14*(23), 6183. https://doi.org/10.3390/rs14236183

Calvari, S., Salerno, G. G., Spampinato, L., Gouhier, M., La Spina, A., Pecora, E., et al. (2011). An unloading foam model to constrain Etna's 11–13 January 2011 lava fountaining episode. *Journal of Geophysical Research*, *116*(B11), B11207. https://doi.org/10.1029/2011JB008407

Cappello, A., Bilotta, G., & Ganci, G. (2022). Modeling of geophysical flows through GPUFLOW. *Applied Sciences*, *12*(9), 4395. https://doi.org/10.3390/app12094395

Cappello, A., Ganci, G., Bilotta, G., Herault, A., Zago, V., & Del Negro, C. (2019). Satellite-driven modeling approach for monitoring lava flow hazards during the 2017 Etna eruption. *Annals of Geophysics*, *62*, VO227.

Carey, S. N., & Sparks, R. S. J. (1986). Quantitative models of the fallout and dispersal of tephra from volcanic eruption columns. *Bulletin of Volcanology*, *48*(2–3), 109–125. https://doi.org/10.1007/bf01046546

Carleo, L., Bonaccorso, A., Currenti, G., & Sicali, A. (2022). Near real-time filtering of high precision borehole strainmeter signals for volcano surveillance. *Annals of Geophysics*, *65*(4), VO428. https://doi.org/10.4401/ag-8787

Carleo, L., Currenti, G., & Bonaccorso, A. (2023). Clustering of eruptive events from high precision strain signals recorded during the 2020-2022 lava fountains at Etna volcano (Italy). *Natural Hazards and Earth System Sciences*, *23*(5), 1743–1754. https://doi.org/10.5194/nhess-23-1743-2023

Carleo, L., Currenti, G., Bonaccorso, A., & Sicali, A. (2022). Real-time signal processing of high-precision borehole strainmeters at Mt. Etna for volcanic surveillance and eruptive events detection. *Il Nuovo Cimento - B C*, *45*(6), 1–4. https://doi.org/10.1393/ncc/i2022-22185-5

Currenti, G., & Bonaccorso, A. (2019). Cyclic magma recharge pulses detected by high-precision strainmeter data: The case of 2017 inter-eruptive activity at Etna volcano. *Scientific Reports*, *9*(1), 1–7. https://doi.org/10.1038/s41598-019-44066-w

Currenti, G., Zuccarello, L., Bonaccorso, A., & Sicali, A. (2017). Borehole volumetric strainmeter calibration from a nearby seismic broadband array at Etna Volcano. *Journal of Geophysical Research: Solid Earth*, *112*(10), 7729–7738. https://doi.org/10.1002/2017JB014663

De Gori, P., Giampiccolo, E., Cocina, O., Branca, S., Doglioni, C., & Chiarabba, C. (2021). Re-pressurized magma at Mt. Etna, Italy, may feed eruptions for years. *Communications Earth & Environment*, *2*(1), 216. https://doi.org/10.1038/s43247-021-00282-9

Engwell, S. L., Aspinall, W. P., & Sparks, R. S. J. (2015). An objective method for the production of isopach maps and implications for the estimation of tephra deposit volumes and their uncertainties. *Bulletin of Volcanology*, *77*(7), 61. https://doi.org/10.1007/s00445-015-0942-y

Ganci, G., Bilotta, G., Zuccarello, F., Calvari, S., & Cappello, A. (2023). A multi-sensor satellite approach to characterize the volcanic deposits emitted during Etna's lava fountaining: The 2020–2022 study case. *Remote Sensing*, *15*(4), 916. https://doi.org/10.3390/rs15040916

Ganci, G., Cappello, A., Bilotta, G., Corradino, C., & Del Negro, C. (2019). Satellite-based reconstruction of the volcanic deposits during the December 2015 Etna eruption. *Data*, *4*(3), 120. https://doi.org/10.3390/data4030120

Ganci, G., Cappello, A., Bilotta, G., Hérault, A., Zago, V., & Del Negro, C. (2018). Mapping volcanic deposits of the 2011–2015 Etna eruptive events using satellite remote sensing. *Frontiers of Earth Science*, *6*, 83. https://doi.org/10.3389/feart.2018.00083

Ganci, G., Cappello, A., & Neri, M. (2023). Data fusion for satellite-derived earth surface: The 2021 topographic map of Etna Volcano. *Remote Sensing*, *15*(1), 198. https://doi.org/10.3390/rs15010198

Ganci, G., Harris, A. J. L., Del Negro, C., Guehenneux, Y., Cappello, A., Labazuy, P., et al. (2012). A year of lava fountaining at Etna: Volumes from SEVIRI. *Geophysical Research Letters*, *39*(6), L06305. https://doi.org/10.1029/2012GL051026

Ganci, G., James, M. R., Calvari, S., & Del Negro, C. (2013). Separating the thermal fingerprints of lava flows and simultaneous lava fountaining using ground-based thermal camera and SEVIRI measurements. *Geophysical Research Letters*, *40*(19), 5058–5063. https://doi.org/10.1002/grl.50983

Mahon, K. I. (1996). The New "York" regression: Application of an improved statistical method to geochemistry. *International Geology Review*, *38*(4), 293–303. https://doi.org/10.1080/00206819709465336

NASEM - National Academies of Sciences, Engineering, and Medicine. (2017). *Volcanic eruptions and their repose, unrest, precursors, and timing*. The National Academies Press. https://doi.org/10.17226/24650

Nuth, C., & Kääb, A. (2011). Co-registration and bias corrections of satellite elevation data sets for quantifying glacier thickness change. *The Cryosphere*, *5*(1), 271–290. https://doi.org/10.5194/tc-5-271-2011

Roeloffs, E. A., & Linde, A. T. (2007). Borehole observations of continuous strain and fluid pressure. In *Volcano deformation* (pp. 305–322). https://doi.org/10.1007/978-3-540-49302-0_9

Rupnik, E., Daakir, M., & Pierrot Deseilligny, M. (2017). MicMac – A free, open-source solution for photogrammetry [Software]. Open geospatial data, softw. stand., *2*(1), 14. https://doi.org/10.1186/s40965-017-0027-2

Sacks, S. I., Suyehiro, S., Evertson, D. W., & Yamagishi, Y. (1971). Sacks-evertson strainmeter, its installation in Japan and some preliminary results concerning strain steps. *Papers in Meteorology and Geophysics*, *22*(3–4), 195–208. https://doi.org/10.2467/mripapers1950.22.3-4_195

Sparks, R. S. J., Bursik, M. I., Carey, S. N., Gilbert, J. S., Glaze, L. S., Sigurdsson, H., & Woods, A. W. (1997). *Volcanic plumes* (p. 574). Wiley.

Wilson, L., Parfitt, E. A., & Head, J. W., III. (1995). Explosive volcanic eruptions-VIII. The role of magma recycling in controlling the behaviour of Hawaiian-style lava fountains. *Geophysical Journal International*, *121*(1), 215–225. https://doi.org/10.1111/j.1365-246x.1995.tb03522.x